

1
2
3
4
5
6
7
8
9
10
11
12
13

Synoptic variability in the tropical oceanic moist margin

C. M. Robinson^{1,2}, S. Narsey⁴, C. Jakob^{1,2,3}

¹School of Earth, Atmosphere & Environment, Monash University, Clayton, Victoria, Australia

²ARC Centre of Excellence for Climate Extremes, Monash University, Clayton, Victoria, Australia

³ARC Centre of Excellence for the Weather of the 21st Century, Monash University, Clayton, Victoria, Australia

⁴Bureau of Meteorology, Melbourne, Victoria, Australia

Key Points:

- The moist margin displays strong variance on synoptic scales, and its movement is strongly related to precipitation variability.
- Variability in the moist margin is related to mid-tropospheric humidity, and is uncorrelated with sea surface temperature.

Corresponding author: Corey Robinson, corey.robinson@monash.edu

Abstract

Recent research has described a ‘moist margin’ in the tropics, defined through a total column water vapor (TCWV) value of 48 kg m^{-2} , that encloses most of the rainfall over the tropical oceans. Diagnosing the moist margin in the ERA5 reanalysis reveals that it varies particularly on synoptic time scales, which this study aims to quantify. We define ‘wet and dry perturbation’ objects based on the margin’s movement relative to its seasonal climatology. These perturbations are associated with a variety of features, such as tropical cyclones and lows, tropical waves, and extrusions of moisture towards the extratropics. Wet (dry) perturbations produce substantially more (less) rainfall compared to the seasonal average, confirming the clear link between moisture and precipitation. On synoptic scales we suggest that mid-tropospheric humidity plays a key role in creating these perturbations, while sea surface temperatures (SSTs) are relatively unimportant.

Plain Language Summary

Rainfall over the tropical oceans tends to be confined within a large-scale, highly humid region enclosed by the ‘moist margin’. This work aims to describe how the moist margin varies from one day to another. We find that shifts of the moist margin strongly control rainfall variability around the boundary of the tropics. Therefore, understanding the processes leading to shifts in the moist margin is an important component of understanding precipitation variability. We suggest that water vapor in the middle levels of the atmosphere, rather than sea surface temperatures, play a key role in controlling the moist margin.

1 Introduction

Water vapor is a key ingredient for moist convection and precipitation, particularly in the tropics where the Coriolis force is small and horizontal temperature gradients are generally weak. The relationship between moisture and precipitation has long been studied in a range of contexts from convective modeling and parameterizations to large-scale variability and anthropogenic climate change (Arakawa & Schubert, 1974; Kain & Fritsch, 1990; Sherwood, 1999; Holloway & Neelin, 2009; Sherwood et al., 2010). There is a well-documented nonlinear relationship between total column water vapor (TCWV) and precipitation over tropical oceans, including the ‘convective pickup’ where precipitation rapidly increases above a critical humidity threshold (Zeng, 1999; Bretherton et al., 2004; Peters & Neelin, 2006; Holloway & Neelin, 2009; Neelin et al., 2009; Ahmed & Schumacher, 2015; Schiro et al., 2016; Virman et al., 2018). Despite this, even areas deemed suitable for heavy convection still exhibit large variability on multiple spatial and temporal scales (Muller et al., 2009; Stechmann & Neelin, 2011; Gilmore, 2015).

A recent study by Mapes et al. (2018) defines the tropical ‘moist margin’ as a sharp boundary at a TCWV value of 48 kg m^{-2} over the oceans. This boundary separates broad areas of a wet regime, where heavy rainfall sporadically occurs, from a dry regime where rainfall is suppressed. Simple observation of the moist margin on synoptic scales demonstrates its ‘meandering’ behavior through time and space. This includes excursions of the wet regime towards higher latitudes, and incursions of dry air into the deep tropics. The movement of the moist margin is therefore expected to change the region where heavy convective rainfall is permitted.

However, no comprehensive analysis of the variability of the tropical moist margin has been performed. Therefore, this study seeks to extend on the work of Mapes et al. (2018) by examining how the tropical moist margin varies on synoptic scales. An object-based approach will be taken here to define perturbations of the moist margin from its basic seasonal cycle.

The paper will be structured as follows. Section 2 first describes the observational and reanalysis data used throughout the study. Section 3 then examines the relationship between TCWV and precipitation over tropical oceans in the context of the moist margin, demonstrating the suitability of reanalysis data for analysis of the moist margin. Section 4 presents the main analysis of variability in the moist margin, beginning with the seasonal cycle (part 4.1) and following with synoptic variability (part 4.2). In Section 5, we examine some large-scale conditions associated with wet and dry perturbations, including the vertical structure of the troposphere and sea surface temperatures (SSTs). A discussion and conclusion are presented in sections 6 and 7 respectively.

2 Data

Total column water vapor (TCWV), specific humidity, temperature and vertical motion data are taken from the ERA5 reanalysis, provided by the European Centre for Medium-Range Weather Forecasts (Hersbach et al., 2020). All variables have been re-sampled to daily means over 1979-2021 at 1° horizontal resolution, providing 43 years of data for analysis. Unless otherwise indicated, the analysis is performed between 30°N - S .

Rainfall data is taken from the Global Precipitation Climatology Project (GPCP) version 1.3 (Adler et al., 2020), an observational dataset that provides daily rainfall at 1° resolution, the same as the downsampled ERA5 data. Note that the GPCP record begins in October 1996, so any joint analysis between TCWV and precipitation is taken over the overlapping period Jan 1997 – Dec 2021.

We use daily SST data from the Optimum Interpolation SST version 2.1 (OISST) provided by NOAA (Huang et al., 2021). OISST data has a resolution of 0.25° and begins in September 1981; once again overlapping periods with ERA5 are used.

3 The relationship between total column water vapor, the moist margin, and rainfall in ERA5

In their study, Mapes et al. (2018) used instantaneous satellite-based observations for TCWV. Here, we repeat the analysis with ERA5 by first evaluating the representation of TCWV distributions over the tropical oceans, shown in Figure 1a. A bimodal distribution of TCWV is clearly evident, including a ‘dry mode’ at 30 kg m^{-2} , a ‘moist mode’ at around 55 kg m^{-2} , and a local minimum between the two which defines the ‘moist margin’. Overall, the distribution is remarkably similar to the results of Mapes et al. (2018) (see their Figure 1). Some slight differences exist; for example, the minimum is at a slightly lower value of around 45-46 rather than 48 kg m^{-2} (e.g. for 25°N-S), and the ‘shoulder’ is slightly less clear for narrower latitude bands (e.g. for 15°N-S), picking up at slightly lower values. However, these differences are minor, and we conclude that reanalysis datasets such as ERA5 are suitable for analyzing the moist margin. For all subsequent analysis, we take the moist margin to be the $\text{TCWV} = 48 \text{ kg m}^{-2}$ contour, as in Mapes et al. (2018). We have repeated all analysis with a lower threshold of 45 kg m^{-2} , and the differences in results are minor and qualitatively identical.

Conditionally sampling on the presence of rainfall highly skews the TCWV distribution, as shown in Figure 1b. Even a small rainfall threshold of 1 mm day^{-1} dramatically shifts the distribution to its moist mode and removes a large fraction of TCWV values below 48 kg m^{-2} . This suggests that the ‘dry mode’ is mostly associated with rain-free conditions, and would likely include oceanic desert regions such as the tropical cold tongues and the subtropical high-pressure regions. As the rainfall threshold increases, the distribution becomes more skewed and the TCWV of the moist mode increases slightly, approaching 60 kg m^{-2} . All distributions for TCWV for differing rainfall thresholds become similar beyond around 60 kg m^{-2} , suggesting that high rainfall amounts are as-

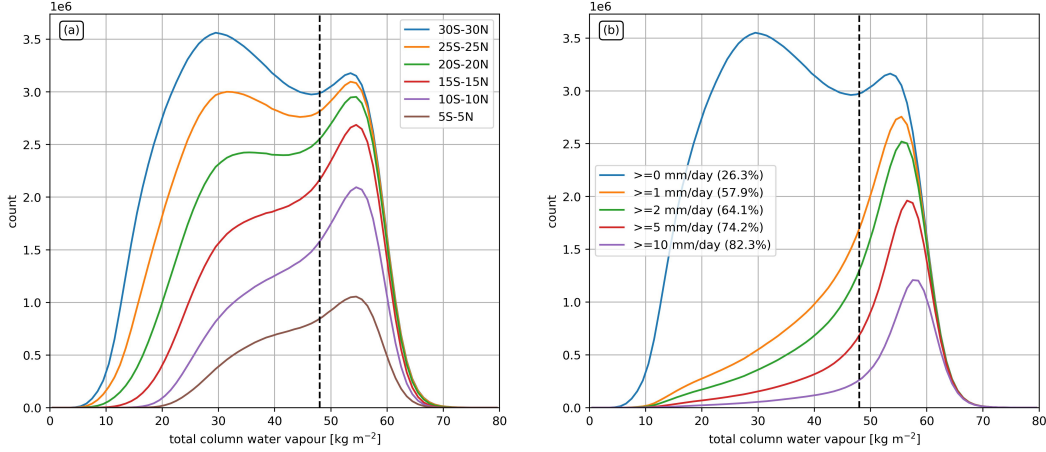


Figure 1. Histogram of ERA5 daily-mean TCWV values over tropical oceans, filtered by latitude band (a) and daily rainfall (b). The moist margin at 48 kg m^{-2} is labelled as the vertical dashed line

112 sociated with the highest TCWV. This is likely because the atmosphere is approaching
 113 its limit of saturation and must therefore produce rainfall. The proportion of TCWV points
 114 above 48 kg m^{-2} increases from 57.9% at 1 mm day^{-1} to 82.3% at 10 mm day^{-1} , both
 115 of which are well above the unconditional value of 26.3%. However, heavy rainfall still
 116 occasionally occurs at low TCWV values, which may be due to strong dynamical forc-
 117 ing, for example through the intrusion of extratropical Rossby waves into the tropics (Kiladis
 118 & Weickmann, 1992) or development of land-sea breezes (Bergemann & Jakob, 2016).

119 Overall, this section supports the idea that being inside the moist margin is an im-
 120 portant but insufficient condition for heavy rainfall over tropical oceans. The next sec-
 121 tion examines how this margin and therefore the region in which heavy rainfall occurs
 122 evolves through time.

123 4 Variability in the moist margin

124 4.1 Seasonal cycle

125 We begin by investigating the seasonal cycle of the moist margin. Figure 2 shows
 126 the position of the moist margin along with the mean TCWV and variance for all months
 127 (top), austral summer (middle), and boreal summer (bottom). In the annual mean, the
 128 margin is confined within 20° N-S , displaying multiple climatic features such as the trop-
 129 ical warm pool over the Maritime Continent, and the intertropical convergence zones (ITCZ)
 130 over the Pacific and Atlantic Oceans. A strong monsoonal migration is evident, partic-
 131 ularly the Asian-Australian monsoon which migrates from northern Australia during aus-
 132 tral summer to India and Southeast Asia in the boreal summer. Seasonal differences are
 133 also present in the western Indian Ocean, which is only covered by the margin during
 134 austral summer, and the central Pacific, which is only continuously inside the margin
 135 during boreal summer. The South Pacific convergence zone (SPCZ) is also somewhat
 136 evident as a southward extension of the margin near the dateline, particularly during aus-
 137 tral summer.

138 It is important to note that the use of ERA5 allows us to also display the moist
 139 margin over land, while the original definition of the moist margin is only over oceans
 140 (Mapes et al., 2018). The applicability of the 48 kg m^{-2} contour over land is therefore

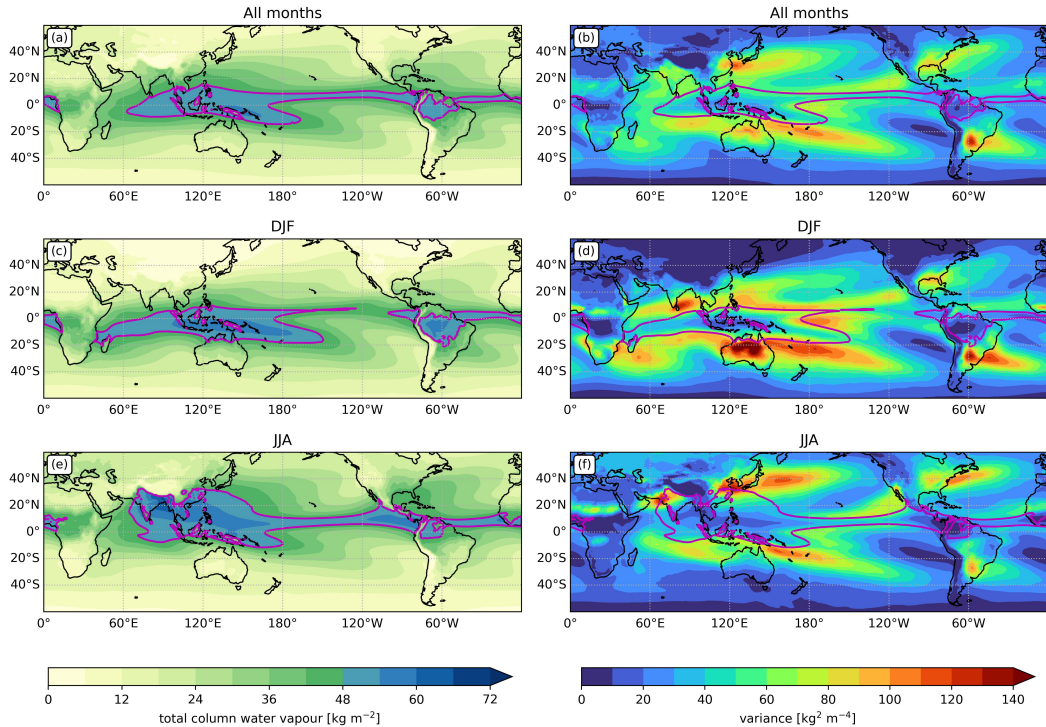


Figure 2. TCWV mean (left) and daily variance (right) for all months (top), DJF (middle), and JJA (bottom). The purple contour in all panels denotes the moist margin at 48 kg m^{-2} .

141 an open question. Interestingly, the moist margin is clearly identifiable over South Amer-
 142 ica, but is absent over tropical Africa, indicating important differences in the rainfall be-
 143 havior over the two continents. This will be further discussed in Section 6.1.

144 The daily variance plots in Figure 2 show that variability is largest in the regions
 145 straddling the edges of the mean moist margin in all seasons. This suggests that these
 146 areas are hotspots for activity on synoptic and longer timescales. Interestingly, the SPCZ
 147 and other diagonal convergence zones are even more easily identifiable in the variance
 148 compared to the mean state. This suggests that these climatic features are the result of
 149 transient activity rather than mean conditions, consistent with dynamical studies of the
 150 SPCZ (Matthews, 2012; van der Wiel et al., 2015). Also prominent are the dominant tracks
 151 for tropical lows and cyclones in the Northwest Pacific and North Atlantic, as well as north-
 152 central Australia and south-central South America. The former is likely due to moisture
 153 variations between tropical disturbances such as cyclones and the clear periods between,
 154 while the large variance over Australia during austral summer may indicate the strong
 155 disparity between monsoon burst and break conditions (Troup, 1961; Pope et al., 2009;
 156 Berry & Reeder, 2016; Narsey et al., 2017)

157 Areas inside the climatological margin tend to have smaller variance, and are there-
 158 fore more consistently humid compared to regions outside the margin. This allows us
 159 to create a conceptual framework where the area contained by the margin acts like a reser-
 160 voir of moisture (i.e. the ‘deep tropics’), where moisture is high and variability is small.
 161 Transient activity periodically moves this moisture to higher latitudes outside the cli-
 162 matological margin, which is interspersed by dry periods, creating high TCWV variance.
 163 This will be further analyzed in the next section.

164

4.2 Synoptic variability

165

166

167

168

169

170

171

172

173

174

As stated in the introduction, strong ‘meanders’ in the moist margin can be observed in snapshots of TCWV, and understanding its movement provides the main motivation for this study. An example of this for 28 Jan 2019 is shown in Figure 3a. Here, the margin shows considerable perturbations from the basic austral summer state shown in Figure 2c. This includes features such as Tropical Cyclone Riley in the southeast Indian Ocean, a monsoon low over northeast Australia, a frontal-like structure on the southwest Indian Ocean with a dry intrusion to its east, and a wet-dry-wet wave pattern in the West Pacific in both hemispheres. The overlaid rainfall in Figure 3a shows that it is mostly confined to areas within the margin, with some exceptions. Possible reasons for these exceptions are further discussed in Section 6.1.

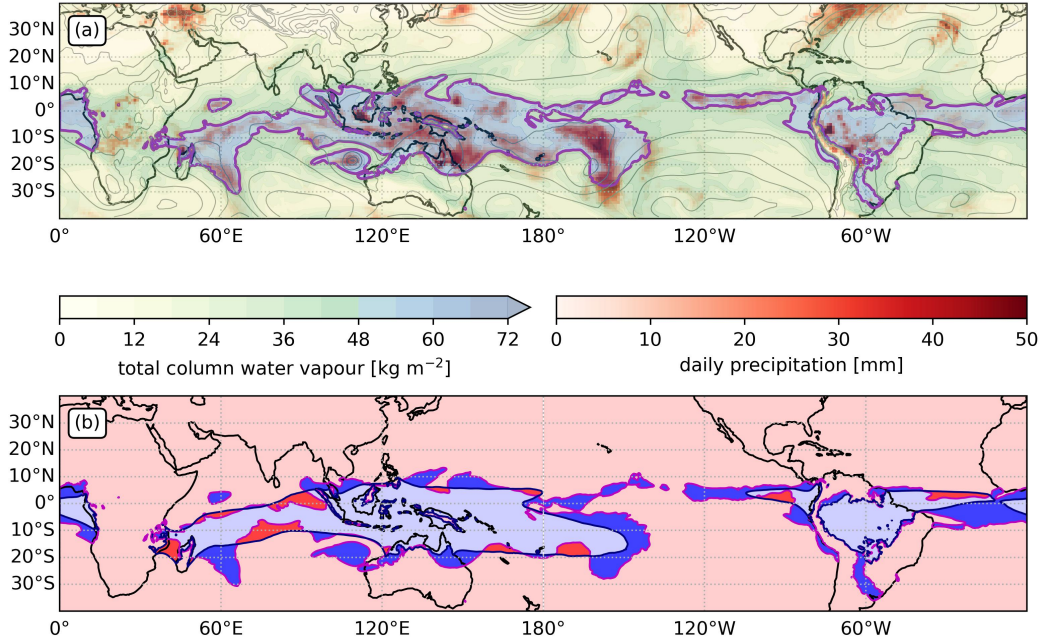


Figure 3. Daily mean TCWV (shading), moist margin (purple contour), mean sea level pressure (thin gray contours) and precipitation (red shading) for 28 Jan 2019 (a). Corresponding moisture categories are shown in panel b, where the navy contour denotes the basic state moist margin. Wet perturbations are in dark blue, dry perturbations are in dark red, wet normal is in light blue, and dry normal is in light red.

175

4.2.1 Wet and dry perturbations

176

177

178

179

To effectively analyze the synoptic variability of the moist margin, we seek a method to define anomalously wet and dry areas. We create four categories based on the movement of the margin in relation to its annual cycle, calculated as a centered 15-day moving average over 1979-2021:

180

181

182

183

1. ‘Wet perturbations’ are areas above 48 kg m^{-2} that are below in the climatology,
2. ‘Dry perturbations’ are areas below 48 kg m^{-2} that are above in the climatology,
3. ‘Wet normal’ are areas that are above 48 kg m^{-2} at that timestep as well as the climatology,

184 4. ‘Dry normal’ are areas that are below 48 kg m^{-2} at that timestep as well as the
 185 climatology.

186 Figure 3b shows objects for these four categories for 28 Jan 2019. The wet pertur-
 187 bations, shaded in dark blue, are largely outward extensions of the moist margin, and
 188 the dry perturbations, shaded in dark red, are generally inward intrusions of the mar-
 189 gin. Some isolated wet perturbations exist, such as near 60°E , $0\text{--}5^\circ \text{N}$; these have been
 190 termed ‘atmospheric lakes’ by Mapes and Tsai (2021). Heavy rainfall is common in the
 191 wet perturbations (see Figure 3a), and largely absent in the dry perturbations.

192 **4.2.2 Object properties**

193 We now turn our attention to some basic properties of the objects introduced above,
 194 in particular the wet and dry perturbations. Figure 4 shows the frequency of occurrence
 195 of wet and dry perturbations for austral summer (top) and winter (bottom). In the fol-
 196 lowing discussion, note that by definition, wet perturbations must occur outside the cli-
 197 matological margin, and dry perturbations must occur inside it.

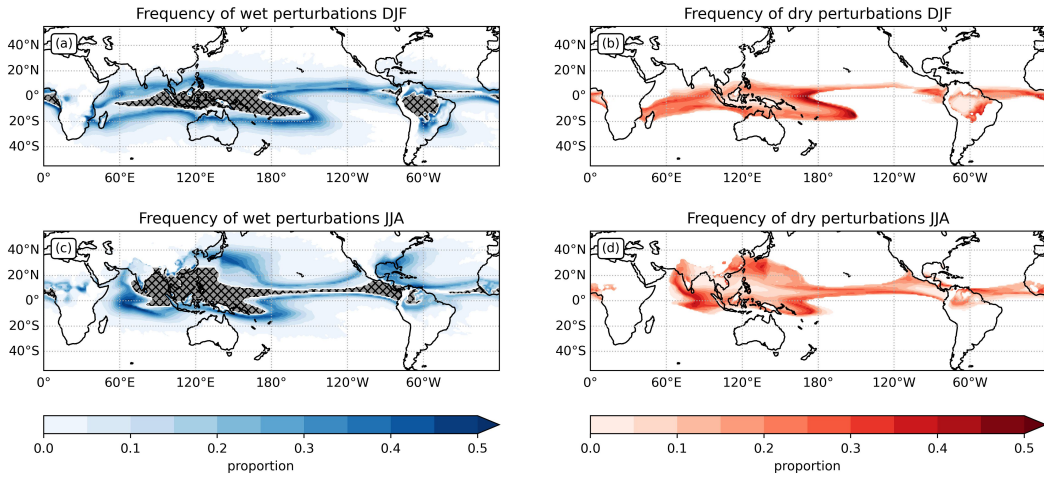


Figure 4. Frequency maps of wet perturbations (left) and dry perturbations (right) for DJF (top) and JJA (bottom). Regions which never experience perturbations are in white. The hatched area in the left panels denote where the climatological TCWV is above 48 kg m^{-2} , and therefore by definition no wet perturbations can occur.

198 Wet perturbations occur most often in the shoulder regions of the tropics, espe-
 199 cially around the ITCZ and SPCZ, and occur less frequently moving away from the cli-
 200 matological margin, which shifts by season. This is unsurprising, as areas close to the
 201 climatological margin would be expected to have TCWV go above 48 kg m^{-2} more of-
 202 ten. Wet perturbations can occasionally extend past 40°N/S in the summer hemisphere,
 203 especially in the Northwest Pacific and North Atlantic. This is likely due to tropical cy-
 204 clones or strong midlatitude interactions which transport tropical moisture to higher lat-
 205 itudes.

206 Dry perturbations are most frequent in regions just inside the climatological moist
 207 margin, particularly around the ITCZ, SPCZ, and central Indian Ocean. Although less
 208 common, they can extend all the way into the central Maritime Continent during aus-
 209 tral summer and the Bay of Bengal and South China Sea during boreal summer. There-
 210 fore, any location inside the climatological moist margin is prone to dry perturbations.

211 Figure 5 shows that there is a clear seasonal cycle of the total area covered by wet
 212 and dry perturbations by month. The summer hemisphere has a greater area covered
 213 by both wet and dry perturbations, peaking in August for the Northern Hemisphere and
 214 March for the Southern Hemisphere. This suggests that there is more synoptic ‘activ-
 215 ity’ in the summer hemisphere; for example, a series of tropical cyclones will create mul-
 216 tiple large wet interspersed by dry perturbations. Wet perturbations also cover a larger
 217 area than dry perturbations; this will be expanded on in the following paragraphs.

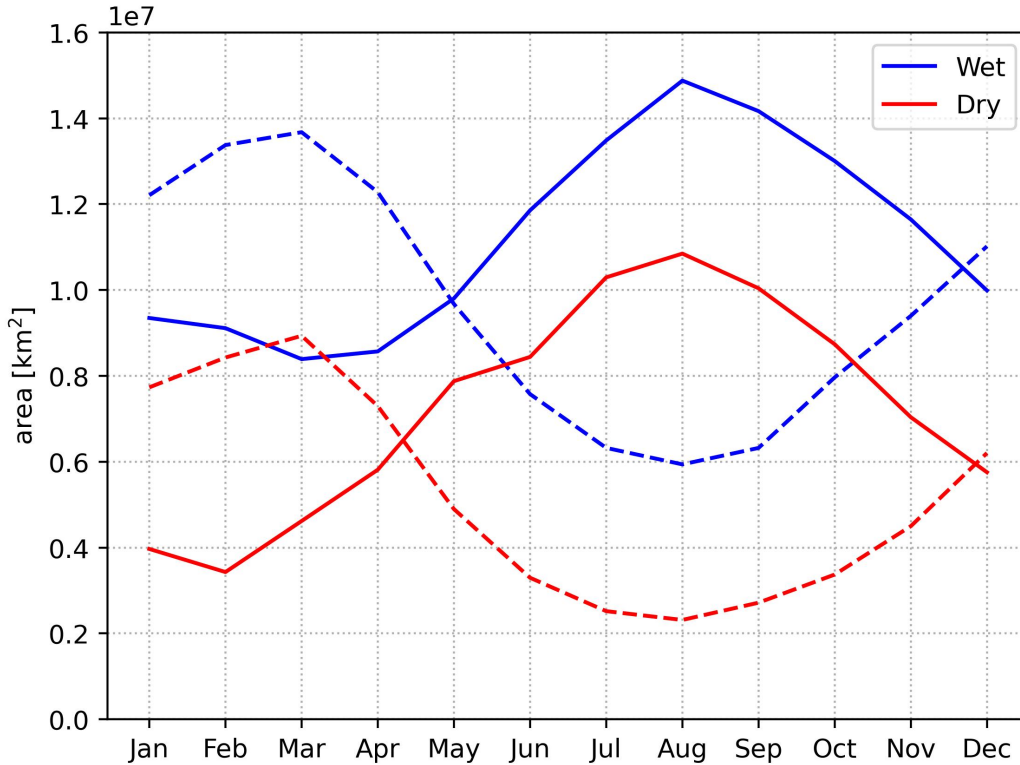


Figure 5. Average area covered by all wet (blue) and dry (red) perturbations in each month by hemisphere. Solid lines show the Northern Hemisphere and dashed lines show the Southern Hemisphere.

218 Figure 6 shows more properties of wet and dry perturbations, including the num-
 219 ber of objects per day, and distributions of object size and mean TCWV anomaly. Note
 220 that in this figure, we have removed all objects smaller than $500,000 \text{ km}^2$, so that we are
 221 only considering large perturbations. In general, there are more wet perturbations (mean
 222 of 10.4) on a given day than dry perturbations (mean of 6.4), though there is consid-
 223 erable spread in the number. Notably, there is always at least one wet and dry perturba-
 224 tion each day.

225 Both wet and dry perturbations have a gamma-like size distribution, meaning there
 226 are many more small objects than large objects. If the minimum area threshold is re-
 227 moved, the distribution keeps the same shape at small sizes (not shown). Although the
 228 distributions for wet and dry perturbations are very similar, there are slightly more large
 229 (above $1 \times 10^6 \text{ km}^2$) wet objects compared to dry objects.

230 Also presented in Figure 6b is the mean TCWV anomaly of wet and dry pertur-
 231 bations, which could be considered a measure of the intensity of the object. Note that

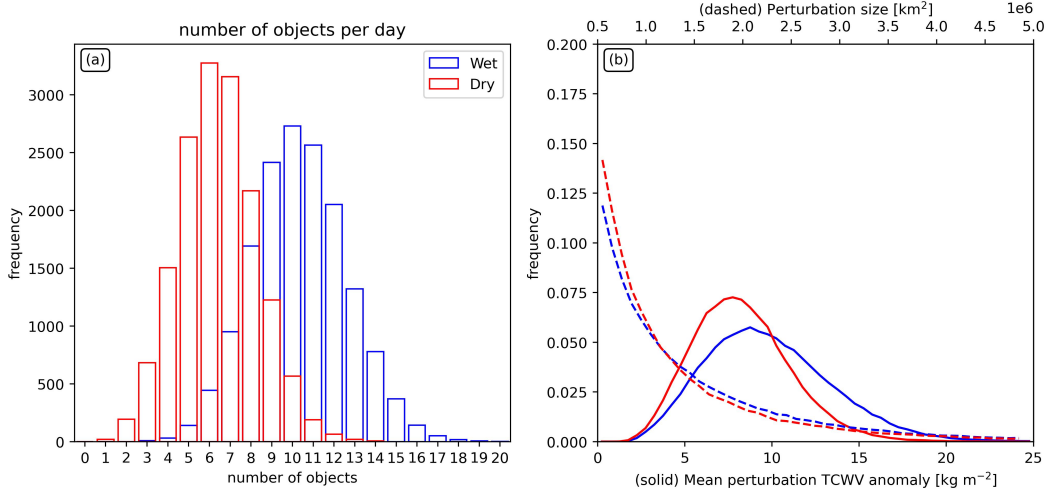


Figure 6. Distributions of the number of objects per day (left), size (right, dashed line) and mean TCWV anomaly (right, solid line) for wet (blue) and dry (red) perturbations. The anomaly for dry perturbations has been multiplied by -1 to make it a positive number.

232 dry perturbation values have been multiplied by -1 for easier display in the same graph.
 233 The mean TCWV anomaly is near-normally distributed for both wet and dry pertur-
 234 bations, though wet perturbations generally have larger anomalies (mean of 10 kg m⁻²)
 235 compared to dry anomalies (mean of 8.5 kg m⁻²). Wet perturbations also have a more
 236 prominent tail at high TCWV anomalies; for example, an anomaly of 15 kg m⁻² is much
 237 more common for wet perturbations compared to dry perturbations.

238 Overall, Figure 6 shows that wet perturbations are typically more frequent, larger,
 239 and more intense than dry perturbations. While this may seem contradictory at first glance,
 240 note that the calculations determining wet and dry perturbations are done by grid point.
 241 Therefore, a balance between wet and dry perturbations at a single snapshot is not re-
 242 quired; rather, there must be a balance between the four categories (including ‘wet nor-
 243 mal’ and ‘dry normal’) at each grid point. Wet perturbations being more frequent and
 244 intense is also consistent with large TCWV variability outside the margin, as shown in
 245 Figure 2. This implies that areas outside the margin are prone to strong undulations in
 246 TCWV, often pushing them above 48 kg m⁻² and into the wet perturbation category.
 247 Meanwhile, areas inside the margin have smaller undulations and therefore fall below the
 248 48 kg m⁻² and into the dry perturbation category less frequently.

249 **4.2.3 Relation of objects with rainfall**

250 We now demonstrate that wet and dry perturbations are tightly linked with rain-
 251 fall variability on synoptic scales. Figures 7a and b show the proportion of daily rain-
 252 fall associated with wet and dry perturbations. Wet perturbations are associated with
 253 a large amount of rainfall along the shoulder regions of the moist tropics. This includes
 254 the northwest and southern Indian Ocean, northern inland Australia, and around the
 255 edges of the ITCZ and SPCZ. Many of these areas experience greater than 50% of their
 256 total rainfall during wet perturbations. Moving further away from the moist tropics, the
 257 proportion of rainfall during wet perturbations becomes smaller, likely due to the rar-
 258 ity of objects there. Some areas in the deep tropics (e.g. the Maritime Continent) ex-
 259 perience little or no rainfall from wet perturbations; this is due to the climatological TCWV
 260 being above 48 kg m⁻² for much of the year. Very little rainfall is associated with dry

261 perturbations, with less than 10% of rainfall occurring during dry perturbations in most
 262 places.

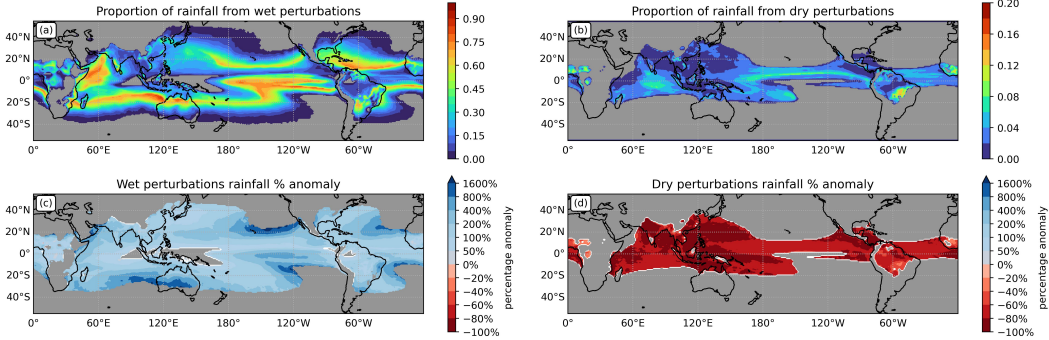


Figure 7. Total proportion of rainfall from wet (a) and dry (b) perturbations. Daily rainfall percentage anomaly compared to the seasonal mean for wet (c) and dry (d) perturbations. Regions where object frequency is below 0.1% are shaded gray. Note the difference in color scales between panels (a) and (b).

263 How large are the rainfall anomalies during wet and dry perturbations? The an-
 264 swer to this likely varies by location. For example, a climatologically dry area may re-
 265 ceive far greater rainfall than usual in a wet perturbation compared to a climatologically
 266 wetter area. Figures 7c and d present daily rainfall percentage anomalies compared to
 267 the 15-day smoothed seasonal climatology. Wet perturbations (Figure 7c) produce over
 268 50% more rainfall compared to climatology across the entire tropics, and this anomaly
 269 increases moving away from the moist tropics and towards drier regions. Some regions
 270 near the equatorial cold tongues and central Australia receive more than 800% of their
 271 mean daily rainfall in a wet perturbation. In comparison, rainfall in the deep tropics is
 272 strongly reduced (less than 40% of usual over most areas) when experiencing a dry per-
 273 turbation. This emphasizes the importance of the moist margin as a strong predictor of
 274 heavy rainfall.

275 **5 Large-scale conditions leading to perturbations**

276 So far, we have presented properties of wet and dry perturbations in the moist mar-
 277 gin, but have not considered the large-scale conditions that these objects form in. In this
 278 section, we will explore what relates to TCWV variance, in particular sea surface tem-
 279 perature and mid-tropospheric humidity.

280 **5.1 Role of sea surface temperatures**

281 Sea surface temperatures (SSTs) may be expected to strongly relate to TCWV, due
 282 to increased evaporation over warm waters. Previous research has shown that low-level
 283 relative humidity over the oceans remains near-constant with global warming, meaning
 284 low-level specific humidity and TCWV closely follows Clausius-Clapeyron scaling with
 285 temperature on long timescales (Trenberth et al., 2005; Sherwood & Meyer, 2006; Held
 286 & Soden, 2006; Willett et al., 2007; Mears et al., 2007; O’Gorman & Muller, 2010). Does
 287 this also apply on synoptic scales?

288 Figure 8 shows 2D histograms of daily-mean SST and TCWV for wet and dry pertur-
 289 bations. There is considerable spread in SST for both wet and dry perturbations, how-
 290 ever, wet perturbations tend to have colder SSTs (mean: 27.7 °C) than dry perturba-

291 tions (mean: 28.6 °C) (Figure 8a). This is the opposite of our hypothesis, which would
 292 predict that wet perturbations tend to occur with *warmer* SSTs. However, the differ-
 293 ence between wet and dry perturbations is simply related to the geographical distribu-
 294 tion of these objects. Wet perturbations occur in the shoulder regions of the tropics, where
 295 SSTs are typically cooler; and dry perturbations occur in the deep tropics, where SSTs
 296 are typically warmer.

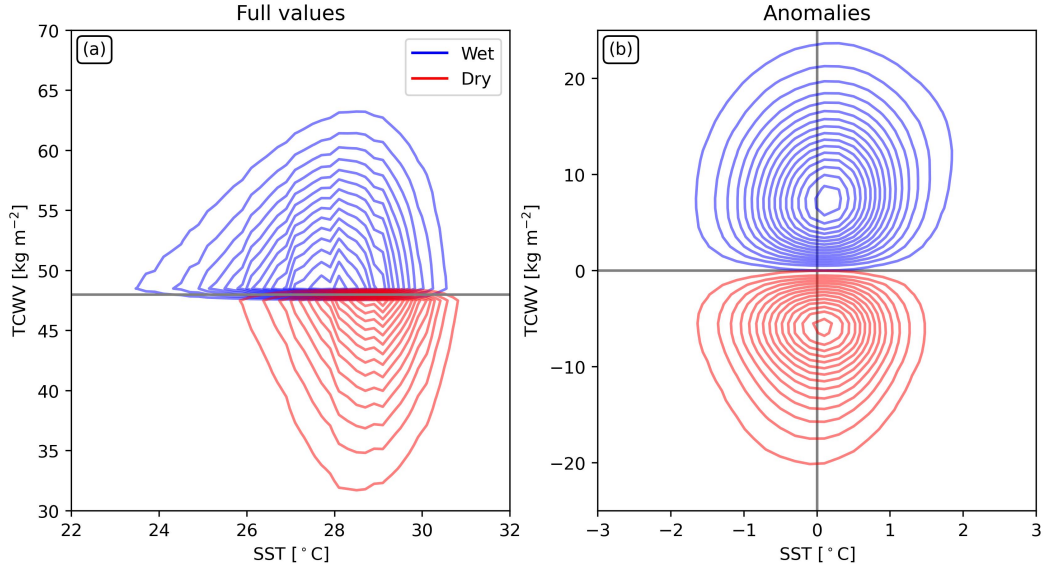


Figure 8. 2D histograms of daily SST and TCWV (a) and their daily anomalies (b), across global tropical oceans (30°N-S). Wet perturbations are in blue and dry perturbations are in red. Each point in the histogram represents one grid point at each time. Histogram spacing is 0.1 K for SST and 1 kg m⁻² for TCWV, and contours are plotted every 10000 points. Note that by definition, wet perturbations must be above 48 kg m⁻² and their anomaly above zero, while dry perturbations must be below 48 kg m⁻² and their anomaly below zero. Therefore, there is no overlap between wet and dry perturbations in the histograms.

297 Removing the climatological SST may better illustrate any relationship between
 298 SST and TCWV, and this is shown in Figure 8b. There is very little difference in the
 299 distribution of SST anomalies between wet (mean: +0.14 °C) and dry perturbations (mean:
 300 -0.03 °C). This suggests that SST anomalies have little to no relationship with TCWV
 301 anomalies and therefore perturbations of the moist margin on daily time scales. This is
 302 in agreement with Neelin et al. (2009), who show that SSTs are unimportant for the con-
 303 vective pickup of rainfall over tropical oceans. TCWV variance must therefore be related
 304 to internal atmospheric processes.

305 5.2 Vertical structure of wet and dry perturbations

306 Figure 9 shows composite profiles of specific humidity, temperature, and vertical
 307 motion anomalies for the four categories described in Section 4.2. In general, wet and
 308 dry perturbations have the strongest anomalies, while ‘wet normal’ and ‘dry normal’ (i.e.
 309 areas above/below 48 kg m⁻² at that timestep as well as the climatology) have weaker
 310 anomalies of the same sign. This is because the wet normal category has dry perturba-
 311 tions removed, meaning the average will be wetter than all times. The opposite is also
 312 true for the dry normal category.

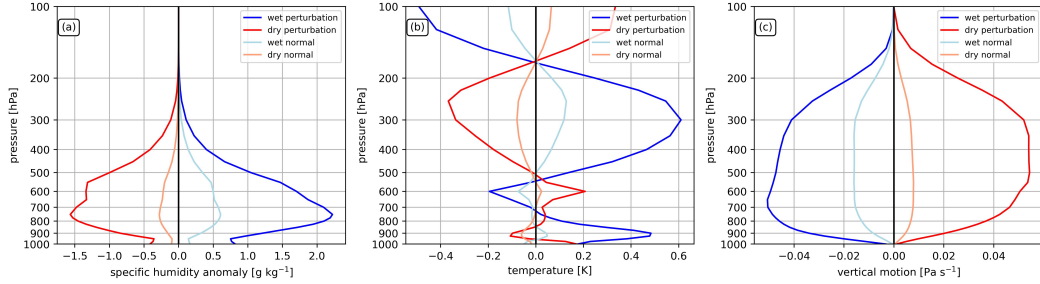


Figure 9. Composite profile of the specific humidity (a), temperature (b), and vertical motion (c) anomalies from the 15-day smoothed seasonal climatology for the four categories described in Section 4.2 within 30°N-S.

313 Wet perturbations are anomalously moist through the whole troposphere, with the
 314 largest anomalies from around 500-900 hPa and a maximum at 750 hPa of 2.2 g kg^{-1} .
 315 Anomalies at 1000 hPa are smaller at 0.8 g kg^{-1} , and near-zero above 250 hPa where
 316 specific humidity is small in all cases. Dry perturbations follow a very similar profile but
 317 with the opposite sign to wet perturbations, having a broader peak of around -1.5 g kg^{-1}
 318 from 800-550 hPa. These results show that the largest differences in humidity between wet
 319 and dry perturbation exist in the mid-troposphere. This is consistent with a wide
 320 body of literature emphasizing the importance of mid-tropospheric moisture for heavy
 321 rainfall from the convective and mesoscale (Brown & Zhang, 1997; Sherwood, 1999; Der-
 322 byshire et al., 2004; Louf et al., 2019) to synoptic (Smith et al., 2015; Ditchek et al., 2016)
 323 and seasonal scales (Parker et al., 2016).

324 To further investigate the likely predominant source of mid-level humidity, we an-
 325alyze the vertical motion profiles shown in Figure 9b. These show upward anomalies for
 326 wet perturbations and downward anomalies for dry perturbations through the whole tro-
 327 posphere. Wet perturbations peak at lower levels (700 hPa) than dry perturbations (500
 328 hPa), both with values of about 0.05 Pa s^{-1} . Stronger upward motion in the wet per-
 329 turbations is consistent with enhanced precipitation and a moister mid-troposphere via
 330 vertical moisture advection. Similarly, subsidence in the dry perturbations is consistent
 331 with reduced precipitation and a drier mid-troposphere. This suggests that vertical ad-
 332 vection is a key source of moisture in the mid-troposphere. However, note that vertical
 333 advection cannot change the full column-integrated specific humidity (i.e. TCWV), and
 334 that changes in TCWV must be due to low-level horizontal convergence and advection.

335 Insight can also be gained from the temperature profiles shown in Figure 9c. The
 336 temperature has a more complex structure comprising multiple peaks and sign changes.
 337 Wet perturbations are anomalously warm in the lower troposphere (1000-700 hPa), anoma-
 338 lously cool in a shallow layer from 700-550 hPa, warm in a deep layer from 550-150 hPa,
 339 and cold above. Dry perturbations again have a very similar profile but in reverse, ex-
 340 cept for the lower-troposphere which has weak and variable temperature anomalies. These
 341 profiles bear a remarkable similarity to a result of Virman et al. (2018) (see their Fig-
 342 ure 2), who suggest that the mid-tropospheric cold anomaly in rainy areas is due to strong
 343 evaporation below the cloud base, which induces subsidence and creates a warm anomaly
 344 at lower levels. This is despite the difference in filtering methods for the composites (we
 345 use TCWV anomalies, while Virman et al. (2018) use absolute rainfall thresholds). The
 346 temperature profiles are also consistent with the archetypal mesoscale convective sys-
 347 tem view of Houze (1989, 1997), where subsidence occurs below the cloud base of strat-
 348 iform regions. Therefore, this appears to be a robust result when comparing wet and dry
 349 areas of the oceanic tropics.

350 6 Discussion

351 6.1 Evaluating the moist margin in the ERA5 reanalysis

352 We have analyzed the variability of the moist margin, defined as $TCWV = 48 \text{ kg}$
 353 m^{-2} , across multiple time scales. We have shown that the ERA5 reanalysis reproduces
 354 features of the TCWV distribution observed in satellite-based products by Mapes et al.
 355 (2018) and is therefore a suitable dataset to analyze the margin.

356 The moist margin is strongly associated with heavy rainfall over the tropical oceans,
 357 although there are some notable exceptions. Figure 3, along with other snapshots, shows
 358 that rainfall often occurs outside the margin, most notably along frontal features in the
 359 winter hemisphere subtropics. These discrepancies are likely related to temperature dif-
 360 ferences across latitudes. For a given TCWV, a colder atmosphere, such as that of the
 361 winter hemisphere subtropics, will be closer to saturation and therefore more likely to
 362 precipitate. Dynamical effects are also more likely to play an important role in organiz-
 363 ing rainfall at higher latitudes, especially along the fronts present in Figure 3.

364 Considering the above, an alternative to TCWV would be to use a variable which
 365 scales with temperature. One example commonly used in the literature is the saturation
 366 fraction, defined as the ratio of vertical integrals of specific humidity to saturation spe-
 367 cific humidity, as a kind of ‘column relative humidity’. Bretherton et al. (2004) found
 368 that the relationship between humidity and mean rainfall over tropical oceans collapses
 369 onto a single curve when using saturation fraction rather than TCWV as the indepen-
 370 dent variable. However, Peters and Neelin (2006) and Neelin et al. (2009) find that the
 371 critical value for convective pickup still depends on temperature. Therefore, accurately
 372 accounting for the temperature dependence on the humidity-precipitation relationship
 373 is difficult. Another complication is that adding temperature-dependence makes for more
 374 difficult prognostic analysis. For example, while changes to TCWV are simple to under-
 375 stand through the moisture budget, changes to saturation fraction or a similar quantity
 376 will also depend on temperature and are not described by one simple equation. Further-
 377 more, snapshots of saturation fraction are noisier and do not depict a clean line in the
 378 tropics (not shown), making it difficult to distinguish between the moist tropics and ex-
 379 tratropics. For these reasons, we choose TCWV as being the most suitable measure for
 380 defining the tropical margin.

381 Our analysis has also shown that the moist margin covers land regions, most promi-
 382 nently over the Amazon in South America, but also over regions such as northern Aus-
 383 tralia, the Maritime Continent, and Southeast Asia. However, the margin is conspicu-
 384 ously absent over Africa. The role of moisture on convection is more complicated over
 385 land due to additional forcings such as topography (Smith et al., 2009; Kirshbaum & Smith,
 386 2009), strong diurnal heating (Nesbitt & Zipser, 2003), and coastal features such as land-
 387 sea breezes (Bergemann & Jakob, 2016). Topography also reduces the depth of the moist
 388 layer, resulting in lower TCWV. However, research has suggested that both the Maritime
 389 Continent and Amazon display ‘oceanic-like’ behavior, and that the convective pickup
 390 first noted over oceans (Peters & Neelin, 2006; Neelin et al., 2009) also applies over these
 391 areas (Schiro et al., 2016; Ahmed & Schumacher, 2017). On the other hand, Africa has
 392 more topography which can interfere with the predominantly easterly synoptic flow and
 393 its associated rainfall (Jackson, 1947). Despite this, sharp humidity gradients such as
 394 the Congo Air Boundary (Howard & Washington, 2019) and Sahel inter-tropical front
 395 (Vizy & Cook, 2017) are features over Africa that control areas of heavy rainfall, act-
 396 ing in a very similar way to the moist margin. Caution is therefore needed when ana-
 397 lyzing the moist margin over land, though we suggest it is still of value.

398 Other differences with Mapes et al. (2018) and similar studies which use high-resolution
 399 observational datasets is the coarser resolution used in our analysis (1° daily means), which
 400 may be expected to alter the relationship of the moist margin with precipitation. Schiro

et al. (2016) find that the convective pickup relationship is robust when averaging to 3-hourly data at 2.5° resolution. Averaging beyond this smooths the relationship and slightly reduces the threshold. This implies that the spatial resolution of 1° in this study is adequate, though the low temporal resolution of 24 hours may suggest a threshold slightly lower than 48 kg m^{-2} may be more suitable for the moist margin, consistent with the slightly lower TCWV values seen in Figure 1 compared to Mapes et al. (2018).

Some limitations of the moist margin method include:

1. The moist margin breaks up over land, most notably Africa, and does not capture all rainfall at higher latitudes, particularly in the winter hemisphere.
2. There is still considerable variability within the moist margin, and 48 kg m^{-2} threshold is not a sufficient condition for heavy rainfall. Dynamical factors leading to uplift are another vital component for rainfall.
3. Climate models are poor at representing the moist margin (and more generally, the relationship between moisture and precipitation), as shown in Mapes et al. (2018). Therefore, caution is needed when analyzing the moist margin in models.

6.2 What creates wet and dry perturbations?

The synoptic variability of the margin has been analyzed with ‘wet and dry perturbation’ objects, defined in Section 4.2. These objects occur in the shoulder regions of the deep tropics, which has a strong seasonal migration towards the summer hemisphere.

Wet perturbations likely encompass a variety of dynamical features, including tropical cyclones and lows, tropical waves, as well as atmospheric rivers (Zhu & Newell, 1998; Gimeno et al., 2014), tropical plumes (Knippertz, 2007), tropical moisture exports (Knippertz & Wernli, 2010; Knippertz et al., 2013), and their related synoptic systems. Some of these features are likely due to strong extratropical interactions with the moist margin. One notable area for this is the SPCZ and SACZ, where research has shown that rainfall variability is influenced by extratropical Rossby waves that refract towards the tropics and cause dynamical uplift leading to rainfall (Matthews, 2012; van der Wiel et al., 2015).

Dry perturbations bear a natural resemblance to the ‘dry intrusions’ commonly described in the literature. Dry intrusions generally form through the descent and advection of dry air from the subtropics to the tropics and are also tightly linked to midlatitude processes (Mapes & Zuidema, 1996; Yoneyama & Parsons, 1999; Casey et al., 2009; Raveh-Rubin, 2017; Aslam et al., 2023). Clearly, extratropical dynamics are an important factor for driving variability in the moist margin and creating both wet and dry perturbations. Further investigation of this will be the subject of future research.

Are variations in humidity at the moist margin purely driven by synoptic dynamics, or does moisture itself play a role in producing variability? Theories of ‘moisture modes’ suggest that moisture, rather than temperature, is the key factor controlling large-scale wave dynamics (Raymond & Fuchs, 2007; Adames et al., 2019). Wave-like structures in the moist margin are common, for example in the Southwest Pacific in Figure 3, suggesting a natural link with moisture mode theory. These structures may also include convectively coupled equatorial waves (Wheeler & Kiladis, 1999; Kiladis et al., 2009). However, we leave detailed analysis of this to future work.

7 Conclusion

This study has analyzed the synoptic variability of the moist margin and related it to rainfall and other large-scale conditions in the tropics. The moist margin is a useful measure that relates tropical precipitation variability to tropical moisture over oceans,

448 since it largely bounds heavy rainfall. This defines the ‘moist tropics’ where heavy rain-
449 fall is most likely to occur.

450 The moist margin exhibits a strong seasonal cycle, particularly in monsoonal re-
451 gions. Wet and dry perturbations, defined through the movement of the margin relative
452 to its seasonal climatology, are strongly linked to rainfall variability along the shoulder
453 regions of the moist tropics. These perturbations are most related to mid-tropospheric
454 humidity and have little to no correlation with SSTs.

455 The objects analyzed here may be linked to a variety of processes, such as trop-
456 ical waves, the Madden-Julian Oscillation, synoptic weather systems such as tropical lows
457 and cyclones, and midlatitude influences. Future work in this topic will explore the dy-
458 namical causes, evolution, and decay of synoptic disturbances of the moist tropical mar-
459 gin. This likely requires tracking the objects through time and space, and the use of prog-
460 nostic analysis such as the moisture and circulation budgets.

461 Open Research Section

462 Data from the ERA5 reanalysis is obtainable from the ECMWF Copernicus Cli-
463 mate Data Store (<https://cds.climate.copernicus.eu/cdsapp#!/home>). GPCP rain-
464 fall data was received from NCAR at <https://rda.ucar.edu/datasets/ds728.7/>. Data
465 from OISST is available at [https://www.ncei.noaa.gov/products/optimum-interpolation-
466 -sst](https://www.ncei.noaa.gov/products/optimum-interpolation-sst). The code used to generate all plots is in Python.

467 Acknowledgments

468 This research is supported by the Australian Research Council Centre of Excellence for
469 Climate Extremes (CE170100023), the ARC Centre of Excellence for the Weather of the
470 21st Century (CE230100012), and the ARC Discovery Project (DP200102954). We ac-
471 knowledge the National Computational Infrastructure for their provision of computa-
472 tional resources and services.

473 References

- 474 Adames, Á. F., Kim, D., Clark, S. K., Ming, Y., & Inoue, K. (2019). Scale analysis
475 of moist thermodynamics in a simple model and the relationship between mois-
476 ture modes and gravity waves. *Journal of the Atmospheric Sciences*, *76*(12),
477 3863–3881.
- 478 Adler, R., Wang, J.-J., Sapiano, M., Huffman, G., Bolvin, D., Nelkin, E., & NOAA
479 CDR Program. (2020). *Global precipitation climatology project (gpcp) climate
480 data record (cdr), version 1.3 (daily)*. Boulder CO: Research Data Archive
481 at the National Center for Atmospheric Research, Computational and Infor-
482 mation Systems Laboratory. Retrieved from [https://doi.org/10.5065/
483 ZGJD-9B02](https://doi.org/10.5065/ZGJD-9B02)
- 484 Ahmed, F., & Schumacher, C. (2015). Convective and stratiform components of the
485 precipitation-moisture relationship [Journal Article]. *Geophysical Research Let-
486 ters*, *42*(23). doi: 10.1002/2015gl066957
- 487 Ahmed, F., & Schumacher, C. (2017). Geographical differences in the tropical
488 precipitation-moisture relationship and rain intensity onset [Journal Article].
489 *Geophysical Research Letters*, *44*(2), 1114–1122. doi: 10.1002/2016gl071980
- 490 Arakawa, A., & Schubert, W. H. (1974). Interaction of a Cumulus Cloud Ensemble
491 with the Large-Scale Environment, Part I [Journal Article]. *Journal of the At-
492 mospheric Sciences*, *31*(3), 674–701.
- 493 Aslam, A. A., Schwendike, J., Peatman, S. C., Birch, C. E., Bolasina, M. A., &
494 Barrett, P. (2023). Mid-Level Dry Air Intrusions over the southern Maritime
495 Continent [Journal Article]. *Quarterly Journal of the Royal Meteorological*

- 496 *Society*. doi: 10.1002/qj.4618
- 497 Bergemann, M., & Jakob, C. (2016). How important is tropospheric humidity for
498 coastal rainfall in the tropics? [Journal Article]. *Geophysical Research Letters*,
499 *43*(11), 5860-5868. doi: 10.1002/2016gl069255
- 500 Berry, G. J., & Reeder, M. J. (2016). The Dynamics of Australian Monsoon Bursts
501 [Journal Article]. *Journal of the Atmospheric Sciences*, *73*(1), 55-69. doi: 10
502 .1175/jas-d-15-0071.1
- 503 Bretherton, C. S., Peters, M. E., & Back, L. E. (2004). Relationships between Water
504 Vapor Path and Precipitation over the Tropical Oceans [Journal Article]. *Jour-
505 nal of Climate*, *17*(7), 1517-1528.
- 506 Brown, R. G., & Zhang, C. (1997). Variability of Midtropospheric Moisture and
507 Its Effect on Cloud-Top Height Distribution during TOGA COARE* [Journal
508 Article]. *Journal of the Atmospheric Sciences*, *54*(23), 2760-2774.
- 509 Casey, S. P. F., Dessler, A. E., & Schumacher, C. (2009). Five-Year Climatology of
510 Midtroposphere Dry Air Layers in Warm Tropical Ocean Regions as Viewed by
511 AIRS/Aqua [Journal Article]. *Journal of Applied Meteorology and Climatology*,
512 *48*(9), 1831-1842. doi: 10.1175/2009jamc2099.1
- 513 Derbyshire, S. H., Beau, I., Bechtold, P., Grandpeix, J. Y., Piriou, J. M., Re-
514 delseperger, J. L., & Soares, P. M. M. (2004). Sensitivity of moist convection
515 to environmental humidity [Journal Article]. *Quarterly Journal of the Royal
516 Meteorological Society*, *130*(604), 3055-3079. doi: 10.1256/qj.03.130
- 517 Ditchek, S. D., Boos, W. R., Camargo, S. J., & Tippett, M. K. (2016). A Genesis
518 Index for Monsoon Disturbances [Journal Article]. *Journal of Climate*, *29*(14),
519 5189-5203. doi: 10.1175/jcli-d-15-0704.1
- 520 Gilmore, J. B. (2015). Understanding the Influence of Measurement Uncertainty
521 on the Atmospheric Transition in Rainfall and Column Water Vapor [Jour-
522 nal Article]. *Journal of the Atmospheric Sciences*, *72*(5), 2041-2054. doi:
523 10.1175/jas-d-14-0211.1
- 524 Gimeno, L., Nieto, R., Vázquez, M., & Lavers, D. A. (2014). Atmospheric rivers: a
525 mini-review [Journal Article]. *Frontiers in Earth Science*, *2*. doi: 10.3389/feart
526 .2014.00002
- 527 Held, I. M., & Soden, B. J. (2006). Robust Responses of the Hydrological Cycle to
528 Global Warming [Journal Article]. *Journal of Climate*, *19*(21), 5686-5699.
- 529 Hersbach, H., Bell, B., Berrisford, P., Hirahara, S., Horányi, A., Muñoz-Sabater,
530 J., ... Thépaut, J.-N. (2020). The ERA5 global reanalysis [Journal Article].
531 *Quarterly Journal of the Royal Meteorological Society*, *146*(730), 1999-2049.
532 doi: 10.1002/qj.3803
- 533 Holloway, C. E., & Neelin, J. D. (2009). Moisture Vertical Structure, Column Wa-
534 ter Vapor, and Tropical Deep Convection [Journal Article]. *Journal of the At-
535 mospheric Sciences*, *66*(6), 1665-1683. doi: 10.1175/2008jas2806.1
- 536 Houze, R. A. (1989). Observed structure of mesoscale convective systems and impli-
537 cations for large-scale heating [Journal Article]. *Quarterly Journal of the Royal
538 Meteorological Society*, *115*(487), 425-461. doi: 10.1002/qj.49711548702
- 539 Houze, R. A. (1997). Stratiform Precipitation in Regions of Convection: A Meteorolo-
540 gical Paradox? [Journal Article]. *Bulletin of the American Meteorological So-
541 ciety*, *78*(10), 2179-2196.
- 542 Howard, E., & Washington, R. (2019). Drylines in Southern Africa: Rediscovering
543 the Congo Air Boundary [Journal Article]. *Journal of Climate*, *32*(23), 8223-
544 8242. doi: 10.1175/jcli-d-19-0437.1
- 545 Huang, B., Liu, C., Banzon, V., Freeman, E., Graham, G., Hankins, B., ... Zhang,
546 H.-M. (2021). Improvements of the Daily Optimum Interpolation Sea Surface
547 Temperature (DOISST) Version 2.1 [Journal Article]. *Journal of Climate*,
548 *34*(8), 2923-2939. doi: 10.1175/jcli-d-20-0166.1
- 549 Jackson, S. P. (1947). Air Masses and the Circulation over the Plateau and Coasts
550 of South Africa [Journal Article]. *South African Geographical Journal*, *29*(1),

- 551 1-15. doi: 10.1080/03736245.1947.10559251
- 552 Kain, J. S., & Fritsch, J. M. (1990). A One-Dimensional Entraining/Detraining
553 Plume Model and Its Application in Convective Parameterization [Journal
554 Article]. *Journal of the Atmospheric Sciences*, *47*(23), 2784-2802.
- 555 Kiladis, G. N., & Weickmann, K. M. (1992). Extratropical Forcing of Tropical Pa-
556 cific Convection during Northern Winter [Journal Article]. *Monthly Weather*
557 *Review*, *120*(9), 1924-1939.
- 558 Kiladis, G. N., Wheeler, M. C., Haertel, P. T., Straub, K. H., & Roundy, P. E.
559 (2009). Convectively coupled equatorial waves [Journal Article]. *Reviews of*
560 *Geophysics*, *47*(2). doi: 10.1029/2008rg000266
- 561 Kirshbaum, D. J., & Smith, R. B. (2009). Orographic Precipitation in the Trop-
562 ics: Large-Eddy Simulations and Theory [Journal Article]. *Journal of the At-*
563 *mospheric Sciences*, *66*(9), 2559-2578. doi: 10.1175/2009jas2990.1
- 564 Knippertz, P. (2007). Tropical-extratropical interactions related to upper-level
565 troughs at low latitudes [Journal Article]. *Dynamics of Atmospheres and*
566 *Oceans*, *43*(1-2), 36-62. doi: 10.1016/j.dynatmoce.2006.06.003
- 567 Knippertz, P., & Wernli, H. (2010). A Lagrangian Climatology of Tropical Moisture
568 Exports to the Northern Hemispheric Extratropics [Journal Article]. *Journal of*
569 *Climate*, *23*(4), 987-1003. doi: 10.1175/2009jcli3333.1
- 570 Knippertz, P., Wernli, H., & Gläser, G. (2013). A Global Climatology of Tropi-
571 cal Moisture Exports [Journal Article]. *Journal of Climate*, *26*(10), 3031-3045.
572 doi: 10.1175/jcli-d-12-00401.1
- 573 Louf, V., Jakob, C., Protat, A., Bergemann, M., & Narsey, S. (2019). The Relation-
574 ship of Cloud Number and Size With Their Large-Scale Environment in Deep
575 Tropical Convection [Journal Article]. *Geophysical Research Letters*, *46*(15),
576 9203-9212. doi: 10.1029/2019gl083964
- 577 Mapes, B., Chung, E. S., Hannah, W. M., Masunaga, H., Wimmers, A. J., & Velden,
578 C. S. (2018). The Meandering Margin of the Meteorological Moist Trop-
579 ics [Journal Article]. *Geophysical Research Letters*, *45*(2), 1177-1184. doi:
580 10.1002/2017gl076440
- 581 Mapes, B., & Tsai, W.-M. (2021, December). Long-lived vapor lakes over the Indian
582 Ocean: closest outdoor phenomenon to the self-aggregation paradigm? In *Agu*
583 *fall meeting abstracts* (Vol. 2021, p. A42B-04).
- 584 Mapes, B., & Zuidema, P. (1996). Radiative-Dynamical Consequences of Dry
585 Tongues in the Tropical Troposphere [Journal Article]. *Journal of the Atmo-*
586 *spheric Sciences*, *53*(4), 620-638.
- 587 Matthews, A. J. (2012). A multiscale framework for the origin and variability of
588 the South Pacific Convergence Zone [Journal Article]. *Quarterly Journal of the*
589 *Royal Meteorological Society*, *138*(666), 1165-1178. doi: 10.1002/qj.1870
- 590 Mears, C. A., Santer, B. D., Wentz, F. J., Taylor, K. E., & Wehner, M. F. (2007).
591 Relationship between temperature and precipitable water changes over trop-
592 ical oceans [Journal Article]. *Geophysical Research Letters*, *34*(24). doi:
593 10.1029/2007gl031936
- 594 Muller, C. J., Back, L. E., O’Gorman, P. A., & Emanuel, K. A. (2009). A model for
595 the relationship between tropical precipitation and column water vapor [Jour-
596 nal Article]. *Geophysical Research Letters*, *36*(16). doi: 10.1029/2009gl039667
- 597 Narsey, S., Reeder, M. J., Ackerley, D., & Jakob, C. (2017). A Midlatitude Influence
598 on Australian Monsoon Bursts [Journal Article]. *Journal of Climate*, *30*(14),
599 5377-5393. doi: 10.1175/jcli-d-16-0686.1
- 600 Neelin, J. D., Peters, O., & Hales, K. (2009). The Transition to Strong Convection
601 [Journal Article]. *Journal of the Atmospheric Sciences*, *66*(8), 2367-2384. doi:
602 10.1175/2009jas2962.1
- 603 Nesbitt, S. W., & Zipser, E. J. (2003). The Diurnal Cycle of Rainfall and Convective
604 Intensity according to Three Years of TRMM Measurements [Journal Article].
605 *Journal of Climate*, *16*(10), 1456-1475.

- 606 O’Gorman, P. A., & Muller, C. J. (2010). How closely do changes in surface and
607 column water vapor follow Clausius-Clapeyron scaling in climate change
608 simulations? [Journal Article]. *Environmental Research Letters*, *5*(2). doi:
609 10.1088/1748-9326/5/2/025207
- 610 Parker, D. J., Willetts, P., Birch, C., Turner, A. G., Marsham, J. H., Taylor, C. M.,
611 ... Martin, G. M. (2016). The interaction of moist convection and mid-level
612 dry air in the advance of the onset of the Indian monsoon [Journal Article].
613 *Quarterly Journal of the Royal Meteorological Society*, *142*(699), 2256-2272.
614 doi: 10.1002/qj.2815
- 615 Peters, O., & Neelin, J. D. (2006). Critical phenomena in atmospheric precipitation
616 [Journal Article]. *Nature Physics*, *2*(6), 393-396. doi: 10.1038/nphys314
- 617 Pope, M., Jakob, C., & Reeder, M. J. (2009). Regimes of the North Australian Wet
618 Season [Journal Article]. *Journal of Climate*, *22*(24), 6699-6715. doi: 10.1175/
619 2009jcli3057.1
- 620 Raveh-Rubin, S. (2017). Dry Intrusions: Lagrangian Climatology and Dynamical
621 Impact on the Planetary Boundary Layer [Journal Article]. *Journal of Cli-*
622 *mate*, *30*(17), 6661-6682. doi: 10.1175/jcli-d-16-0782.1
- 623 Raymond, D. J., & Fuchs, Ž. (2007). Convectively coupled gravity and moisture
624 modes in a simple atmospheric model. *Tellus A: Dynamic Meteorology and*
625 *Oceanography*, *59*(5), 627–640.
- 626 Schiro, K. A., Neelin, J. D., Adams, D. K., & Lintner, B. R. (2016). Deep Con-
627 vection and Column Water Vapor over Tropical Land versus Tropical Ocean:
628 A Comparison between the Amazon and the Tropical Western Pacific [Jour-
629 nal Article]. *Journal of the Atmospheric Sciences*, *73*(10), 4043-4063. doi:
630 10.1175/jas-d-16-0119.1
- 631 Sherwood, S. C. (1999). Convective Precursors and Predictability in the Tropi-
632 cal Western Pacific [Journal Article]. *Monthly Weather Review*, *127*(12), 2977-
633 2991.
- 634 Sherwood, S. C., & Meyer, C. L. (2006). The General Circulation and Robust Relative
635 Humidity [Journal Article]. *Journal of Climate*, *19*(24), 6278-6290.
- 636 Sherwood, S. C., Roca, R., Weckwerth, T. M., & Andronova, N. G. (2010). Tropo-
637 spheric water vapor, convection, and climate [Journal Article]. *Reviews of Geo-*
638 *physics*, *48*(2). doi: 10.1029/2009rg000301
- 639 Smith, R., Montgomery, M. T., Kilroy, G., Tang, S., & Müller, S. K. (2015). Tropi-
640 cal low formation during the Australian monsoon: the events of January 2013
641 [Journal Article]. *Tropical Cyclone Research Report*, *15*(1), 1-18.
- 642 Smith, R., Schafer, P., Kirshbaum, D. J., & Regina, E. (2009). Orographic Precipita-
643 tion in the Tropics: Experiments in Dominica [Journal Article]. *Journal of the*
644 *Atmospheric Sciences*, *66*(6), 1698-1716. doi: 10.1175/2008jas2920.1
- 645 Stechmann, S. N., & Neelin, J. D. (2011). A Stochastic Model for the Transition
646 to Strong Convection [Journal Article]. *Journal of the Atmospheric Sciences*,
647 *68*(12), 2955-2970. doi: 10.1175/jas-d-11-028.1
- 648 Trenberth, K. E., Fasullo, J., & Smith, L. (2005). Trends and variability in column-
649 integrated atmospheric water vapor [Journal Article]. *Climate Dynamics*,
650 *24*(7-8), 741-758. doi: 10.1007/s00382-005-0017-4
- 651 Troup, A. (1961). Variations in upper tropospheric flow associated with the onset of
652 the Australian summer monsoon [Journal Article]. *MAUSAM*, *12*(2), 217-230.
- 653 van der Wiel, K., Matthews, A. J., Stevens, D. P., & Joshi, M. M. (2015). A dy-
654 namical framework for the origin of the diagonal South Pacific and South
655 Atlantic Convergence Zones [Journal Article]. *Quarterly Journal of the Royal*
656 *Meteorological Society*, *141*(691), 1997-2010. doi: 10.1002/qj.2508
- 657 Virman, M., Bister, M., Sinclair, V. A., Järvinen, H., & Räisänen, J. (2018). A New
658 Mechanism for the Dependence of Tropical Convection on Free-Tropospheric
659 Humidity [Journal Article]. *Geophysical Research Letters*, *45*(5), 2516-2523.
660 doi: 10.1002/2018gl077032

- 661 Vizy, E. K., & Cook, K. H. (2017). Mesoscale convective systems and noctur-
662 nal rainfall over the West African Sahel: role of the Inter-tropical front
663 [Journal Article]. *Climate Dynamics*, 50(1-2), 587-614. doi: 10.1007/
664 s00382-017-3628-7
- 665 Wheeler, M. C., & Kiladis, G. N. (1999). Convectively Coupled Equatorial Waves:
666 Analysis of Clouds and Temperature in the Wavenumber-Frequency Domain
667 [Journal Article]. *Journal of the Atmospheric Sciences*, 56(3), 374-399.
- 668 Willett, K. M., Gillett, N. P., Jones, P. D., & Thorne, P. W. (2007). Attribution
669 of observed surface humidity changes to human influence [Journal Article].
670 *Nature*, 449(7163), 710-2. Retrieved from [https://www.ncbi.nlm.nih.gov/
671 pubmed/17928858](https://www.ncbi.nlm.nih.gov/pubmed/17928858) doi: 10.1038/nature06207
- 672 Yoneyama, K., & Parsons, D. B. (1999). A Proposed Mechanism for the Intrusion of
673 Dry Air into the Tropical Western Pacific Region [Journal Article]. *Journal of
674 the Atmospheric Sciences*, 56(11), 1524-1546.
- 675 Zeng, X. (1999). The Relationship among Precipitation, Cloud-Top Temperature,
676 and Precipitable Water over the Tropics [Journal Article]. *Journal of Climate*,
677 12(8), 2503-2514.
- 678 Zhu, Y., & Newell, R. E. (1998). A Proposed Algorithm for Moisture Fluxes from
679 Atmospheric Rivers [Journal Article]. *Monthly Weather Review*, 126(3), 725-
680 735.